10 Experimental Characterization of Phase Transitions

Anna E. Böhmer
Experimental Physics IV
Faculty for Physics and Astronomy
Ruhr University Bochum, 44801 Bochum

Contents

E. Pavarini and E. Koch (eds.)
Correlated Materials: Methods and Applications
Modeling and Simulation Vol. 16, Forschungszentrum Jülich, 2026
ISBN 978-3-95806-909-1 http://www.cond-mat.de/events/correl26

1 Introduction

Phase transitions are an everyday phenomenon. Whether it is the melting of ice cubes, the boiling of water, or the hardening of candle wax, we all experience the sudden change of properties of a material when external conditions (such as the temperature) change. A story on the impact of a structural phase transition concerns the two modifications of Sn: β-Sn is a shiny malleable metal, perfect for making uniform buttons. α-Sn is a gray brittle semiconductor of little use. As the story goes, Napoleon's troops in 1812 marched into freezing Russian winter with temperatures as low as −40°C, where their tin uniform buttons began to disintegrate due to the transition from β-Sn to α-Sn. Without buttons to keep their coats closed, the soldiers could not keep warm and in the end Napoleon lost the campaign.
The phase transitions of correlated materials go far beyond the solid-liquid-gas aggregate states or the different structural modifications of elements and compounds. Typically, we are interested in transitions that arise from electronic or magnetic interactions. One finds diverse subtle structural transitions, but also a rich variety of magnetic phase transitions, transitions to superconductivity and even more exotic phase transitions. Identifying the presence of phase transitions and how they evolve with external "tuning parameters" (control parameters) such as pressure, magnetic field or material composition is a crucial step in understanding a material. Often, only discrete points in a phase diagram can be probed, so establishing a complete phase diagram with areas of different phases bordered by phase lines involves knowledge of constraints for phase diagrams, interpretation, and, sometimes, speculation. In addition to establishing the topology of a phase diagram, the nature of the different phases needs to be determined. This may be straightforward, but can also seem like an impossible problem in some cases. The whole arsenal of solid-state physics is often employed to understand all aspects of the nature of a phase diagram and the individual phases.
In these lecture notes, I will present aspects of the experimental characterization of phase transitions from a personal point of view. I will start with a brief description of what constitutes a phase transition and how phase transitions are classified. I will touch on the important matter of symmetries and constraints for phase diagrams. Second, I will explain how phase transitions can be identified experimentally. As an example, I will discuss the establishing of the temperature-substitution phase diagram of the iron-based material $Ba(Fe_{1-x}Co_x)_2As_2$ and the temperature-pressure phase diagram of FeSe. In the third part of these lecture notes, I will explain some aspects of how the nature of a phase can be determined, with a focus on structural, magnetic, and superconducting phase transitions. The iron-based materials provide again rich examples for the determination of structural and magnetic orders.

2 Background

A phase transition is a consequence of the general tendency of nature to maximize entropy. This is quantified in the general principle of minimization of free energy $F = U - TS$ (or $G = U + pV - TS$). The entropy term dominates at high temperatures and a "disordered" high-

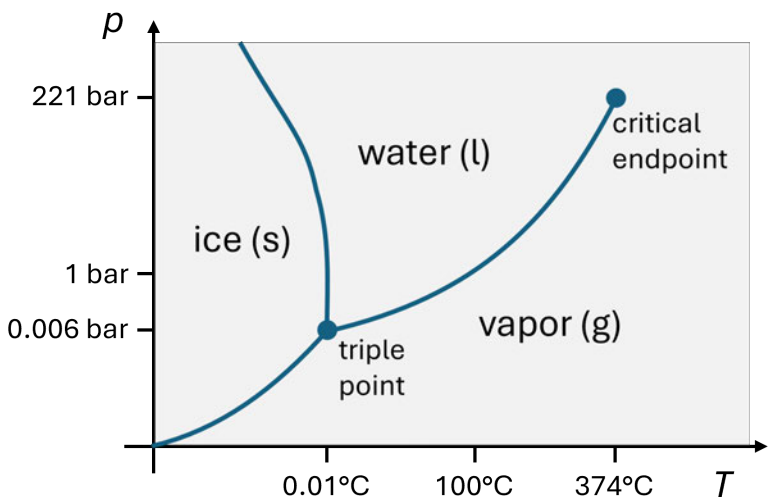

Fig. 1: *The solid (s) - liquid (l) - gas (g) p-T phase diagram of H_2O. Along phase lines, two phases coexist in equilibrium. A phase transition occurs when a line is crossed. At atmospheric pressure of $p = 1$ bar, water vapor condenses into liquid water at 100°C and water freezes into ice at 0°C. At the "triple point", all three phases coexist in equilibrium. The liquid-gas phase line terminates in a "critical endpoint". For pressure/temperature values beyond the critical endpoint, the distinction between liquid and gas vanishes. Figure reproduced from Ref. [2].*

entropy state is preferred. However, if there are states with a lower energy U these will eventually be transitioned into on lowering the temperature. At zero temperature, the entropy term no longer contributes and the ground state of a system is the one with lowest energy.

A phase is defined as a homogeneous region in a material, where intensive variables such as the specific volume, V, specific entropy, S, or particle density, and all of their derivatives vary continuously. However, under certain conditions, the equilibrium state of a material may be the coexistence of different phases. The pressure, p, temperature, T, and chemical potential, μ, of the two phases that are in contact with each other need to be equal. For given p and T, the condition for phase equilibrium is therefore $\mu_1(T, p) = \mu_2(T, p)$. In a p-T diagram (see Fig. 1 for an example), there will be a line along which the two phases may exist in equilibrium. When temperature or pressure are varied such that this line is crossed, a phase transition occurs [1]. During a phase transition, the properties of the material change abruptly. This sudden change of properties is experimentally seen as an "anomaly" in a measured curve (e.g., $V(T)$). Here, we will not discuss situations in which multiple phases coexist in equilibrium, though such situations are very important as well. Indeed, rich effects are observed in situations where the number of phases changes (such as when a solution of table salt in hot water is cooled and salt crystals form).

The Gibbs phase rule governs the possibility of phase coexistence. It says that the number of freely varying intensive variables, F, equals $F = C-P+N+1$, where C is the number of components in a system, P the number of phases, and N the number of different ways of performing work on the system. The phase diagram in Fig. 1 is an example of a single-component system (C=1) with only one way of performing work (pressure-volume work) (N=1), therefore $F = 3-P$. That means the areas in the phase diagram (both pressure and temperature vary

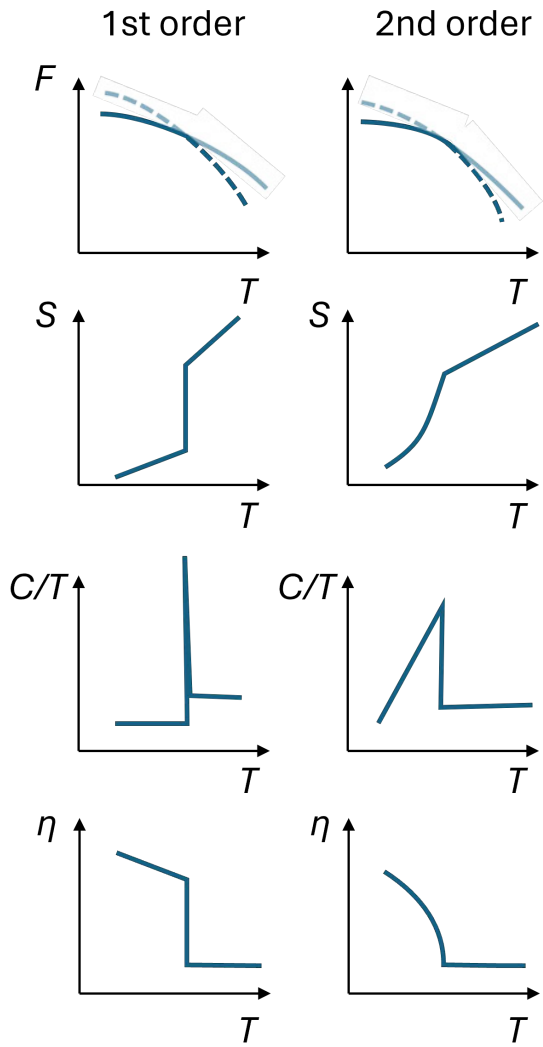

Fig. 2: *Differences between first-order (discontinuous) and second-order (continuous) phase transitions. A first-order phase transition occurs, when the minimum free energy (dark blue) has a slope change, e.g., when the free energies of two phases (indicated as a dashed and a continuous line) cross. The entropy* $S = \frac{\partial F}{\partial T}$ *shows a discontinuity and the heat capacity* $C/T = \frac{\partial S}{\partial T}$ *a delta-type peak. The order parameter assumes a finite value in a discontinuous fashion on entering the ordered phase. At a second-order phase transition, the entropy shows a slope change only, and the heat capacity a discontinuity. The order parameter increases in a continuous fashion.*

freely, F=2) have to be single-phase regions (P=1). Along the phase lines, temperature and pressure are linked, so that F=1 and two phases coexist (P=2). Three phases can coexist, but pressure and temperature cannot vary freely in that case (F=0). This is the triple point.

Phase transitions are classified according to Ehrenfest into different types. A system is described by its free energy F (or G). A phase transition is said to be of first/second order if the first/second derivatives of the free energy show a discontinuity ("a jump" or "step-like anomaly"), respectively. Thus, a phase transition is a mathematical singularity. Any derivative of a thermodynamic potential (such as F or G) is a thermodynamic quantity, and the character of a phase transition is therefore determined by measuring the evolution of thermodynamic quanti-

ties on crossing a phase line (see Fig. 2). First derivatives of the free energy are, e.g., the volume ($V = \partial G/\partial p$), the entropy ($S = -\partial F/\partial T$), or the magnetization ($M = -\partial F/\partial B$, with the appropriate variables held constant in each case). Typically considered second derivatives are the heat capacity $C_p/T = \partial S/\partial T$ or the thermal expansion coefficient $\beta = 1/V\partial V/\partial T$.
Figure 2 presents examples for the anomalies of thermodynamic quantities at first- and second-order phase transitions. A first-order phase transition results in a step in the entropy, which means a delta-like anomaly in the heat-capacity, whereas a second-order phase transition results in a step in the heat capacity, which means a slope change ("kink") in the entropy. The finite entropy change ΔS at a first-order phase transition corresponds to a latent heat $Q = T\Delta S$. It naturally causes a hysteresis, which means that the transitions occurs at a lower temperature on cooling than on heating (or equivalently for other control parameters).
Famously, phase transitions are described in Landau theory, where the free energy is expanded in terms of an "order parameter" that describes the ordered phase. The order parameter is finite only in the ordered phase and reflects all of its symmetry properties. An example is the magnetization of a ferromagnet. In a continuous phase transition, the order parameter increases continuously from zero, whereas in a discontinuous phase transition (only first-order transition), the order parameter abruptly assumes a finite value.
It is important to determine the nature of phase transition (continuous or discontinuous), as many constraints depend it. A phase transition can only be continuous if it breaks one symmetry [3]. Examples are a loss of a C_2 rotation in a tetragonal-to-orthorhombic structural transition, or the loss of time-reversal for a paramagnetic-to-ferromagnetic phase transition. Discontinuous phase transitions may also occur between phases of the same symmetry (e.g., liquid-gas), or change more than one symmetry element. A phase line can terminate in a critical endpoint only if there is no symmetry change between the two phases. In addition, there are multiple constraints on how different phase lines can meet in a phase diagram, see Refs. [4] or [5] for just two examples. Such constraints depend on the type of the phase transitions involved. The constraints can be extremely helpful to complete and understand a phase diagram as, e.g., in Ref. [6].

3 Experimental identification of a phase transition

3.1 General considerations

Many techniques are used to study phase transitions. Typically, a property of the material is measured as a function of an extensive variable, such as electrical resistance as a function of temperature or magnetization as a function of magnetic field. In principle, *all* properties of a system change suddenly when it undergoes a phase transition, which can be seen as an "anomaly" in such data. Therefore, the measurement of any property can indicate a phase transition. Nevertheless, some techniques are better suited to identify the presence of a phase transition than others. This depends on accessibility of the technique, resolution of the technique, ease of use, effort for sample preparation and, of course, whether the anomaly at the

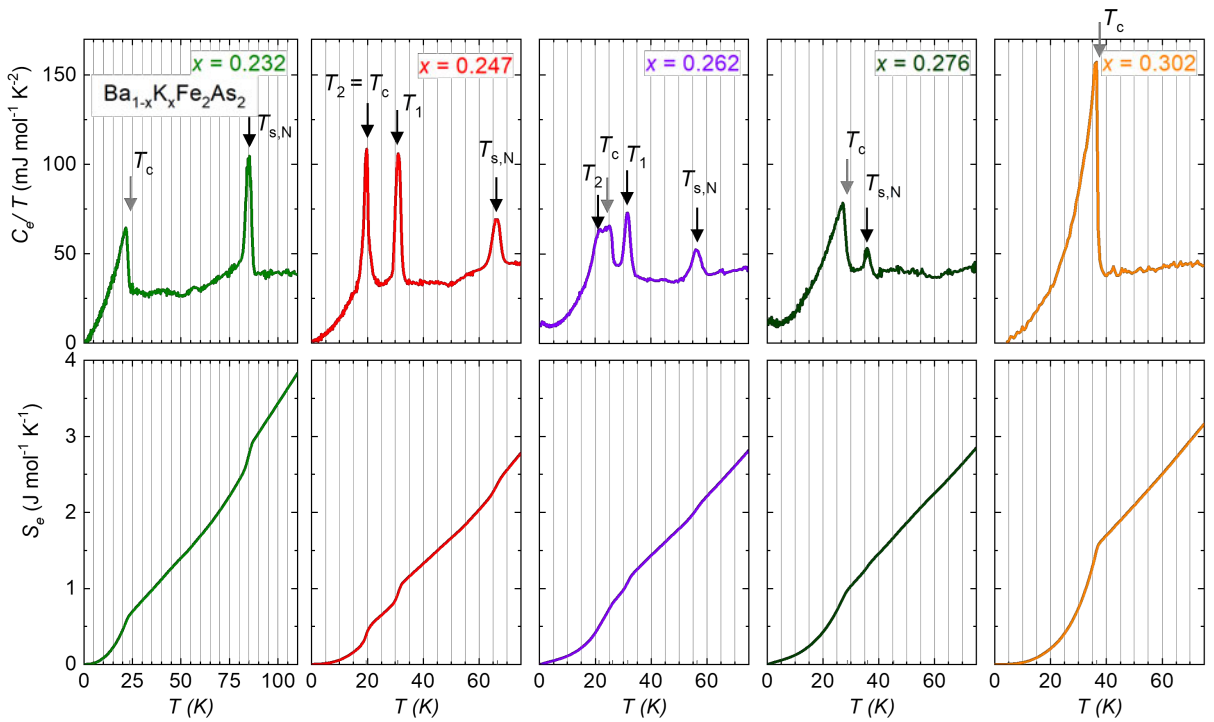

Fig. 3: *Example of the electronic heat capacity of $Ba_{1-x}K_xFe_2As_2$ as a function of temperature. A phonon background has been subtracted from the experimental data and the electronic entropy has been calculated. Various first-order (black arrows) and second-order (grey arrows) phase transitions are observed. All transitions are broadened from an ideal shape to different degrees. Signatures in the entropy can be very subtle. Figure reproduced from [7].*

phase transition is sizable in that specific case. Frequently, the electrical resistance is one of the first quantities measured when one searches for phase transitions. Other typical properties include magnetization, heat capacity, or thermal expansion. For thermodynamic quantities, a second-order phase transition should appear as a kink or step (depending on whether the quantity is a first or second derivative of the free energy). Note that the electrical resistance is a transport property and not a thermodynamic quantity. Therefore, it cannot be used in the same way to make statements about the type of a phase transition. Microscopic or local probes can, of course, also clearly show the onset of some type of order, which is associated with a phase transition. Examples are extremely diverse, such as changes of the diffraction pattern indicating a modification of the crystal structure, signs of the onset of magnetic order in muon spin resonance (μSR), nuclear magnetic resonance (NMR) or Kerr effect, or signatures of inversion symmetry breaking in second harmonic generation in optical systems.

Usually, a phase transition is identified experimentally as a sudden change in the measured property. Figure 3 shows examples of multiple first- and second-order phase transitions as seen in a heat-capacity measurement. In general, phase transitions are never infinitely sharp in experimental data, so what is theoretically a mathematical singularity will be “washed out”. Reasons can be inhomogeneities in the chemical composition of a sample, internal stresses in the sample, or inhomogeneities in the external parameters (e.g., pressure inhomogeneity for a pressure-driven phase transition). Therefore, what is ideally a discontinuity (“a step”) in a

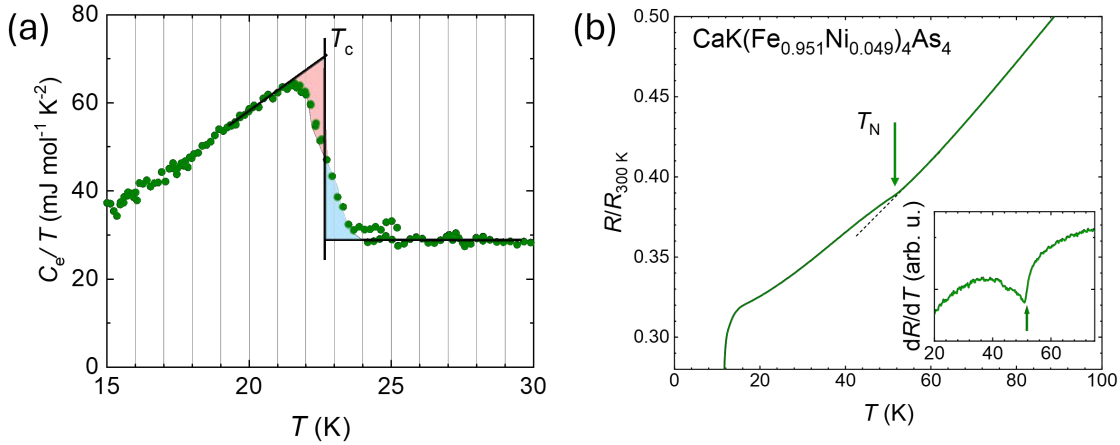

Fig. 4: *(a) The entropy-conserving construction, which is a common criterion for determining the temperature of a second-order phase transition. The areas above and below the idealized curve (read and blue) should be equal. (b) Example of a second-order phase transition in a resistance measurement. In such a transport probe, defining a criterion for a phase transition is not unambiguous. The transition is seen as a deviation from the extrapolated slope of the high-temperature phase (dashed line). A sharp feature is seen in the temperature derivative. (a) based on data in Ref. [7], (b) based on data in Ref. [8].*

measured quantity will become rounded, and a delta-function will become a broadened peak. As a consequence, it is not always easy to distinguish a first-order phase transition from a second-order phase transition in practice. A broadened peak may look not very different from a washed-out step. Typically, if an anomaly looks "symmetric" in rising and falling slope, one would consider the transition to be of first-order. Observation of a hysteresis is a tell-tale sign of a first-order phase transition. However, the absence of an observed hysteresis does not mean that a transition is not first-order. The latent heat may just be too small to cause a significant effect, and most experimental setups cause small differences on heating and cooling anyways, due to the instrumentation.

An additional issue is that, sometimes, a change of properties would occur gradually even in perfect condition and is therefore by definition not a phase transition. It may be called a "crossover" instead. Crossovers may, e.g., be observed beyond the critical endpoint of a first-order phase transition [9]. Due to the presence of intrinsic broadening, it can be difficult to distinguish a true phase transition from a crossover.

A phase transition temperature, T_{crit}, is uniquely defined in the case of an ideally sharp phase transition. In real data, however, one often needs to define a criterion for the T_{crit}. For thermodynamic quantities that show a peak at the phase transition, this is naturally the peak maximum. For step-like anomalies in a thermodynamic quantity (such as C/T at a second-order phase transition), one often defines the mid-point of the step in an "entropy conserving" construction (see Fig. 4). However, if the measured quantity if not a thermodynamic quantity (such as electrical resistance), the criterion can be ambiguous. The more washed out a transition is, the harder T_{crit} is to define. As a general rule, the transition temperature should be taken at the "sharpest feature" in the data. In any case, the criterion should always be defined and stated clearly, and checked for consistency between different publications.

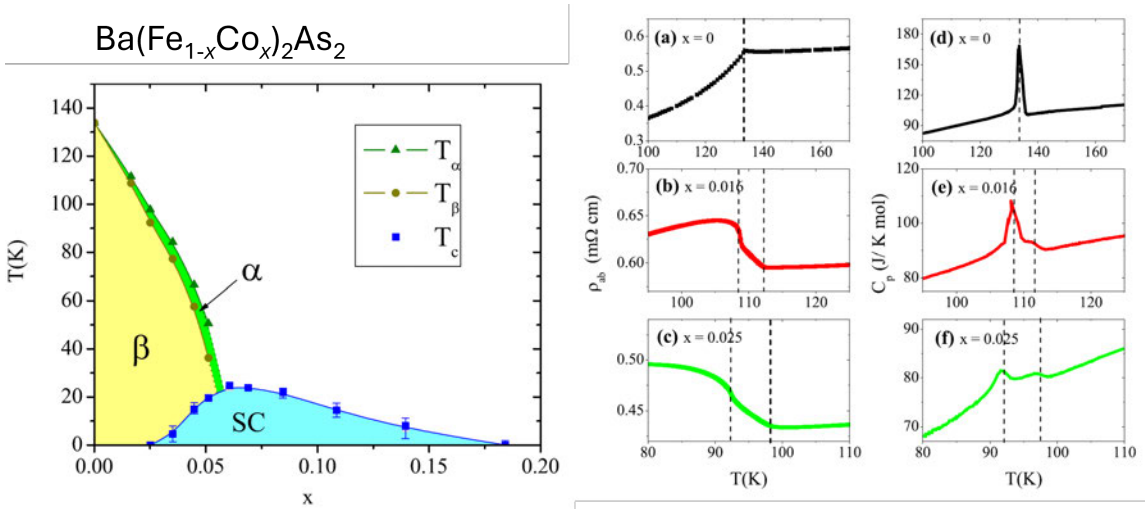

Fig. 5: *Left side: The phase diagram of $Ba(Fe_{1-x}Co_x)_2As_2$. The points are determined from resistivity and heat capacity measurements, examples of which are shown on the right side. For $x = 0$ a single first-order phase transition is observed. For $x = 0.016$ a higher-temperature second-order phase transition is followed by a first-order phase transition at a slightly lower temperature. Figure reproduced from Ref. [12].*

3.2 The phase diagram of iron-based superconductors

High-temperature superconductivity in iron-based compounds was discovered in 2008 [10]. Like many unconventional superconductors, iron-based materials undergo other phase transitions besides superconductivity. Superconductivity arises when these other phase transitions are suppressed to lower temperatures by applied pressure or chemical substitution.

One of the most studied iron-based systems is $Ba(Fe_{1-x}Co_x)_2As_2$. Anomalies in resistance, magnetization, heat capacity and thermal expansion clearly show its phase transitions [11–13] (see Fig. 5). With the thermodynamic probes, the order of the phase transitions can be determined, as explained in the previous section. Indeed, it was found that a first-order transition of the parent compound $BaFe_2As_2$ splits into a second-order phase transition and a lower-temperature first-order phase transition upon Co substitution. For high Co-substitution levels, this lower temperature first-order phase transition changes its character and becomes a second-order phase transition as well. These findings have consequences for theoretical modeling, which was employed, e.g., in Ref. [14, 15].

Identifying a phase transition may be challenging under certain conditions. For example, the available methods are restricted when a transition occurs under applied physical pressure or at extremely low temperatures. As an example, heat capacity measurements under applied pressure are extremely challenging [20]. Also, the sample quality can strongly affect whether a phase transition is visible in a dataset; they may be extremely smeared out so that they are invisible above a background. Some transitions are also genuinely suppressed by disorder in a low-quality sample. For example, superconductivity can be completely destroyed by disorder.

The case of FeSe provides a useful example of the determination of a phase diagram using electrical resistance measurements under pressure (see Fig. 6). Figure 6(e) shows the temperature-

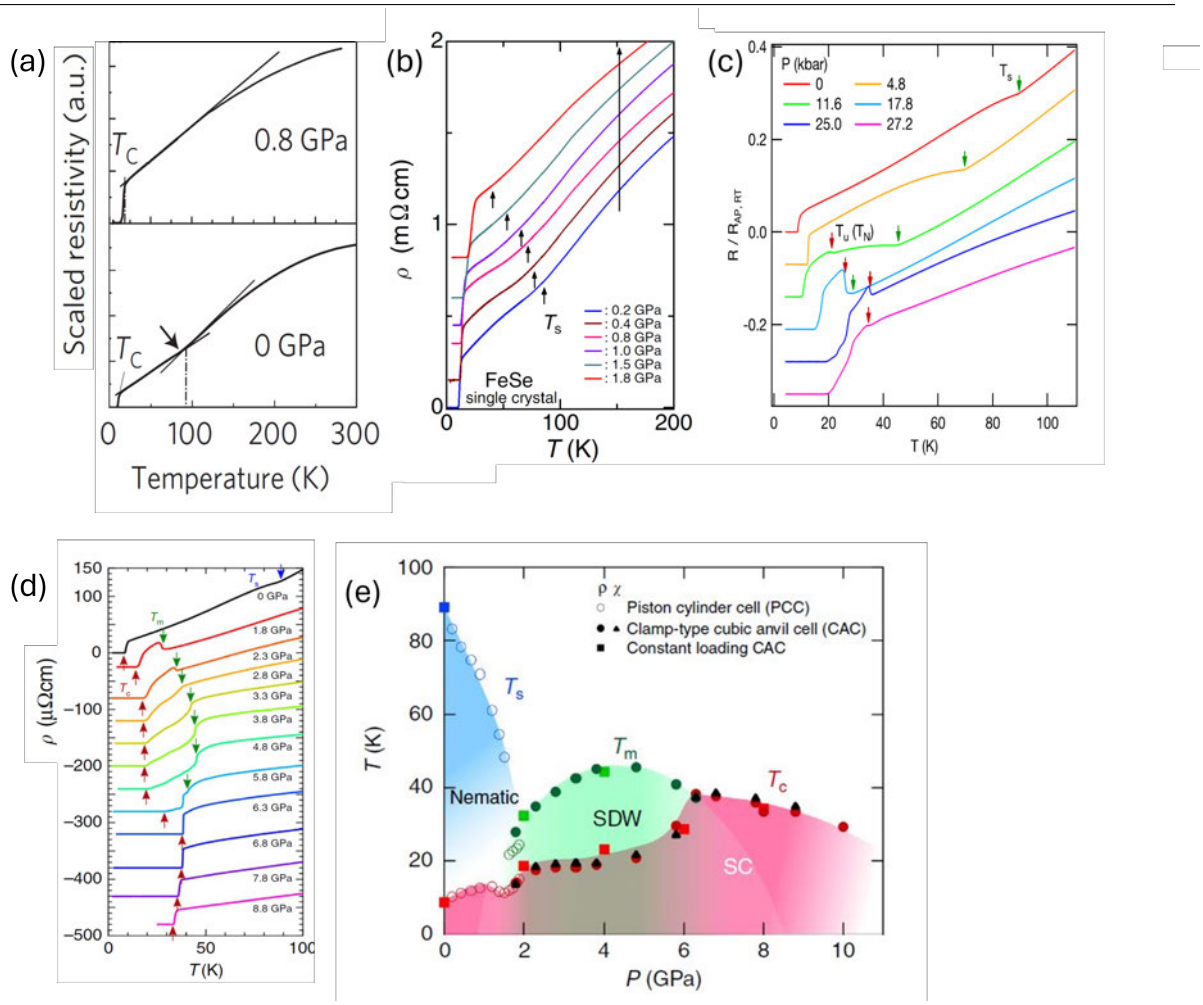

Fig. 6: *Determination of the temperature-pressure phase diagram of FeSe using resistance measurements. In the first dataset in (a), the structural transition is indicated by a slope change slightly below 100 K, but not resolved under applied pressure. In the second dataset in (b), this transition could be followed to higher pressures. In the third dataset in (c), another transition at $T_u(T_N)$ could also be resolved. In (d), data to higher pressures was obtained [T_N is labelled T_m here in (d)], from which the phase diagram in (e) was compiled. (a) reproduced from [16], (b) reproduced from [17], (c) reproduced from [18], (d,e) reproduced [19]*

pressure phase diagram of FeSe. FeSe [21] is an iron-based superconductor whose superconductivity at $T_c = 8$ K was discovered in 2008. FeSe also shows another phase transition at $T_s = 90$ K, whose signature is a subtle kink in resistance. This transition is identified as a tetragonal-to-orthorhombic structural transition via x-ray diffraction and considered an electronically driven nematic transition. Early resistance measurements under pressure showed that the superconducting transition temperature of FeSe increases dramatically up to 40 K at a pressure of ~ 8 GPa. However, the fate of the structural phase transition under pressure was not clear [16]. Surprisingly, μSR first detected the emergence of magnetic order with increasing transition temperature T_N under increasing pressure, where no magnetic order is found at ambient pressure [22]. Several years later, higher-quality samples permitted to follow the resistance anomaly at T_s under pressure, revealing that the structural phase transition was suppressed [17]. But these resistance measurements did not detect any sign of the magnetic phase transition

at T_N. Thus, it was thought possible that the structural and magnetic phase transitions do not occur in the same sample. Only when signatures of both phase transitions were observed in the same measurement [18], it was confirmed that the phase diagram of FeSe under pressure was qualitatively different from the phase diagram of $Ba(Fe_{1-x}Co_x)_2As_2$. Finally, the data were extended to higher pressure ranges [19]. These data revealed that the signature of the magnetic phase transition in resistance measurements changes from an upturn on decreasing temperature to a downturn, respectively (see Fig. 6(e)). Such a change in shape of the resistance anomaly is indeed very much possible as the signature of a transition in electrical transport measurements depends on many microscopic details.

4 Determination of the nature of a phase

Determining the nature of a phase is very much synonymous with identifying its order parameter (or the symmetry changes at the transition). This can be straightforward, or prove to be an almost impossible problem. Some typical questions that need to be answered for the determination of the nature of a phase are:

- Does the ordered phase change the crystal structure, e.g., decrease rotational symmetries of the lattice or reduce translation symmetry (e.g., by doubling a lattice parameter)?
- Is the ordered phase magnetic in nature (thus, break time-reversal symmetry)?
- Is the ordered phase superconducting?

There are cases where the answer is 'none of the above', and a more exotic type of order is realized. Less specific, yet important questions for the characterization of a phase are:

- Does the order parameter correspond to a periodic modulation of a quantity, e.g., a charge-density wave or antiferromagnetism, and which wave-vector $\mathbf{Q}$ characterizes it? Or is the order parameter homogeneous ($\mathbf{Q} = 0$)?
- Is the order even long-range (i.e., the entire sample is well ordered), or does the order only form in "patches" with a limited spatial extent ("correlation length")?

4.1 Experimental techniques for identifying ordered phases

Different techniques are suitable to answer the salient questions on the nature of a phase. Changes in the crystal structure are mainly addressed with diffraction techniques (see Fig. 7). A (slight) distortion of the unit cell, which reduces its symmetry, results in the splitting of a Bragg peak. For example, a tetragonal crystal has only a single in-plane lattice parameter, such that the (200) and (020) Bragg peaks occur at the same diffraction angle. However, in an orthorhombic phase with two distinct in-plane lattice parameters, (200) and (020) occur at different diffraction angles. A change of periodicity, such as the doubling of the unit cell along a specific direction, will lead to the emergence of new "superstructure" diffraction peaks. Diffraction techniques

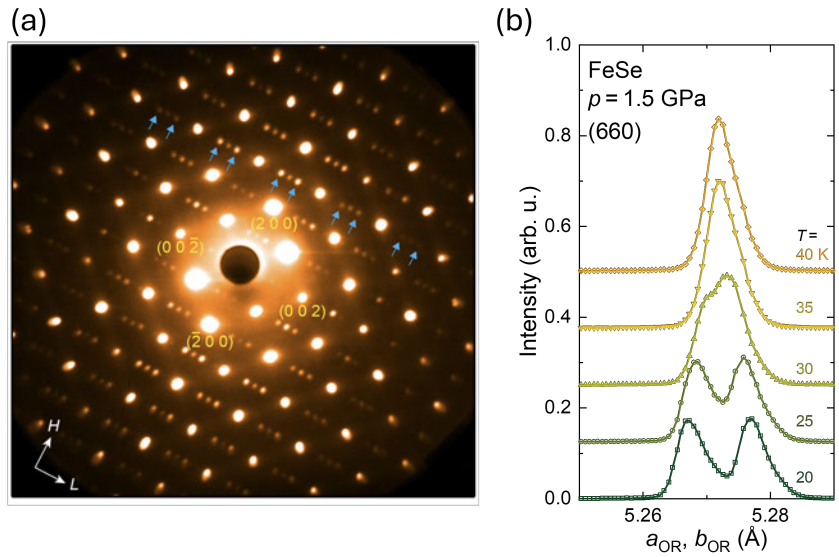

Fig. 7: *Examples of diffraction data revealing a structural phase transition. (a) Diffraction pattern of $LaTe_3$. The small peaks marked by blue arrows (superstructure) result from a charge-density wave transition which leads to an approximate tripling of the c lattice parameter. (b) A distortion of the unit cell can be revealed by a peak splitting. In this case of FeSe at 1.5 GPa of applied pressure, the distortion sets in at approximately 35 K. (a) Reproduced from Ref. [24], (b) based on data in Ref [25].*

can thus inform on the **Q**-vector of an order parameter, as it leads to a periodic modulation, i.e., a superstructure. For example, magnetic diffraction can clarify the wavevector **Q** of an antiferromagnetic order. Diffraction techniques can also inform on a finite correlation length of the order from the peak width, see Ref. [23] for an example.

For magnetic systems, a variety of specialized probes exist. Some techniques are particularly suitable to detect time-reversal-symmetry breaking with very high sensitivity, namely μSR or the magneto-optical Kerr effect. Other techniques probe the periodic internal magnetic fields that arise from the ordered magnetic moments in a crystal ("hyperfine fields"). In techniques such as μSR, NMR, Mössbauer spectroscopy, or ESR, the Zeeman effect of these magnetic fields on a "probe" magnetic moment (implanted muon, nuclear magnetic moment, electron spin) is measured.

Nevertheless, macroscopic techniques that average the entire sample, momentum, and energy are often in the first line when the nature of a phase is studied. Magnetization measurements as a function of temperature and field are extremely useful for characterizing magnetic phases [26, 27], see Fig. 8. A ferromagnetic transition is most clearly revealed by the emergence of finite magnetization on decreasing temperature in a small applied field, whereas the magnetic susceptibility is expected to follow the Curie-Weiss law $\chi = C/(T-T_C)$, with T_C the Curie temperature. An "Arrott-plot" [28] is employed to accurately determine the Curie temperature from magnetization measurements. The ferromagnetic phase is also clearly characterized by its hysteretic response to applied magnetic fields. An antiferromagnetic transition has a classical signature of a cusp in the susceptibility-vs-temperature data and an anisotropic response below this temperature. However, one needs to distinguish materials with localized

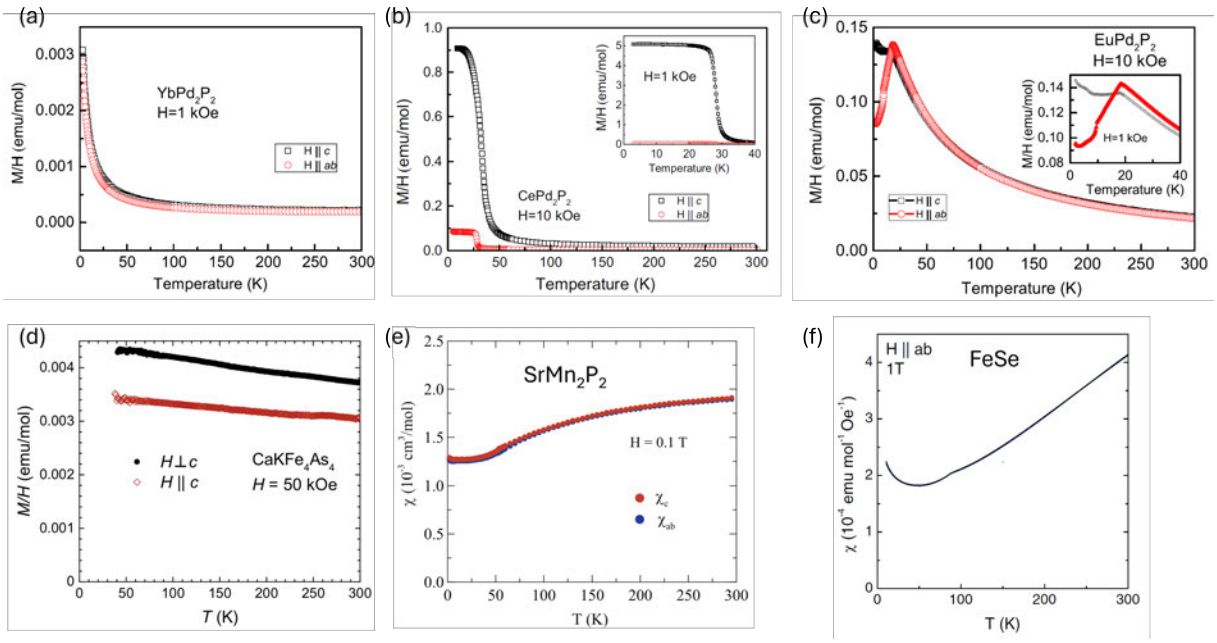

Fig. 8: *Examples of magnetization data. The top row shows magnetic compounds with localized magnetic moments, (a) a paramagnet (b) a ferromagnetic transition at approximately 30 K, (c) an antiferromagnetic transition around 20 K (followed by another transition at lower temperatures). The bottom row shows itinerant magnets, (d) a paramagnet (data below 35 K is missing because the material becomes superconducting below that temperature) and (e) an antiferromagnetic transition. The material in (f) remains paramagnetic at all temperatures and the kink is related to a structural transition. (a-c) reproduced from [29], (d) reproduced from [30], (e) reproduced from [31], (f) reproduced from [32]*

magnetic moments from itinerant magnets (where the magnetic moments are carried by the conduction electrons). In the latter, the magnetic susceptibility can differ dramatically from the localized (textbook-like) behavior and an antiferromagnetic transition can have very different or even extremely subtle signatures. Localized-moment paramagnets, that do not order magnetically, exhibit the characteristic Curie law of the susceptibility $\chi = C/T$, whereas the Pauli paramagnetic susceptibility of conduction electrons is temperature independent in simple cases.

Identifying superconductivity is notorious. Frequently and famously, superconductivity has been reported for materials that turned out not to be superconducting in the end. These include spectacular claims of exceptional high-temperature superconductivity [33], but also other circumstances [34]. The majority of such claims were solid research contributions and the scientific community worked well to confirm or disprove them. On the other hand, superconductivity has also been missed in some instances and rediscovered only years later. The fact that superconductivity has so often been misidentified is intrinsic to its unusual properties. There is a traditional 'triad' of macroscopic experiments, which consists of resistance, magnetic susceptibility and heat capacity measurements, see Fig. 9. Only if the characteristic signatures of superconductivity have been observed in all three experiments, while taking care of the pitfalls of each of the techniques, a well-founded claim that a material is a superconductor can be made.

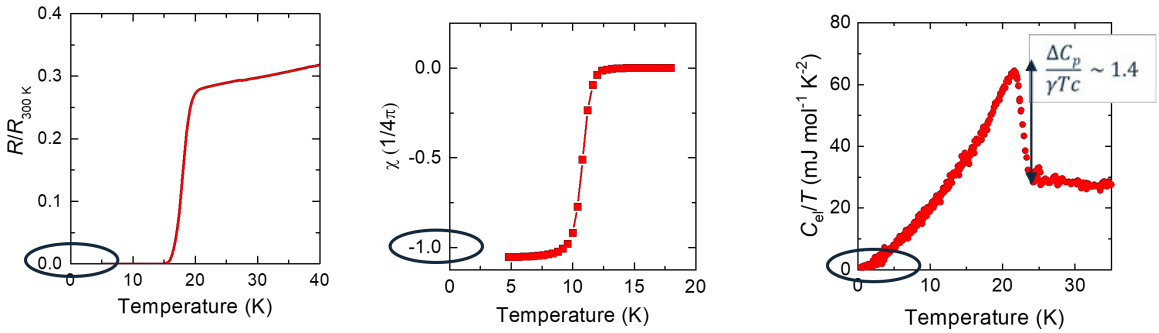

Fig. 9: *The classical three macroscopic experimental results that help identify a superconducting transition. (a) zero resistance, (b) full diamagnetic shielding, (c) sizable heat capacity jump and zero residual heat capacity. (a,b) based on data in Ref. [35], (c) based on data in Ref. [7].*

The observation of zero resistance marked the discovery of superconductivity. Very often, zero resistance (or even a drop of resistance) at a transition temperature T_c that is suppressed in magnetic fields is taken as a signature of superconductivity. In most cases where a new superconducting material is found, this is indeed the starting point. However, different effects play a role. First of all, zero resistance only means that there is one current path which is superconducting. This could be indeed a path along grain boundaries, a distributed minority phase, or even just a sample's surface. Also, a careful four-probe measurement is necessary, to avoid misleading effects when a sample in not homogeneous. However, superconductivity could be missed in resistance measurements in case a material has a very low critical current density that is exceeded in the experiment.

Second, the Meissner effect (a magnetic susceptibility of -1, irrespective of how the superconducting state is reached) is the defining property of a superconductor. Experiments are performed in two manners: 'field cooled', which means that a magnetic field is applied before the sample is cooled through its superconducting transition, or 'zero-field cooled', where a magnetic field is only applied after the sample has been cooled into the superconducting state (see Fig. 10). There are many reasons why a superconductor may not show a susceptibility of -1 experimentally. In many cases, vortex pinning prevents finding a susceptibility of -1 in a field-cooled experiment on a type-II superconductor. Namely, the expulsion of field lines (the epitome of the Meissner effect) does not occur because vortices cannot move freely. For the zero-field cooled experiment, the applied magnetic field needs to be lower than the lower critical field H_{c1} (or the field of first flux penetration) for the susceptibility to reach -1. In new materials, H_{c1} may not be accurately known. On the other hand, demagnetization effects may lead to the observation of a value much smaller than -1. Demagnetization effects are only negligible when a thin plate-like or needle-like sample is measured with field applied along its long dimension. Finally and naturally, the sample mass needs to be sufficiently well known to determine the absolute value of the susceptibility. However, there are cases when this is not possible.

A fundamental effect that limits the conclusions to be drawn from a zero-field cooled magnetization experiment is that only the sample surface is probed. A 'glass ball wrapped in Aluminum'

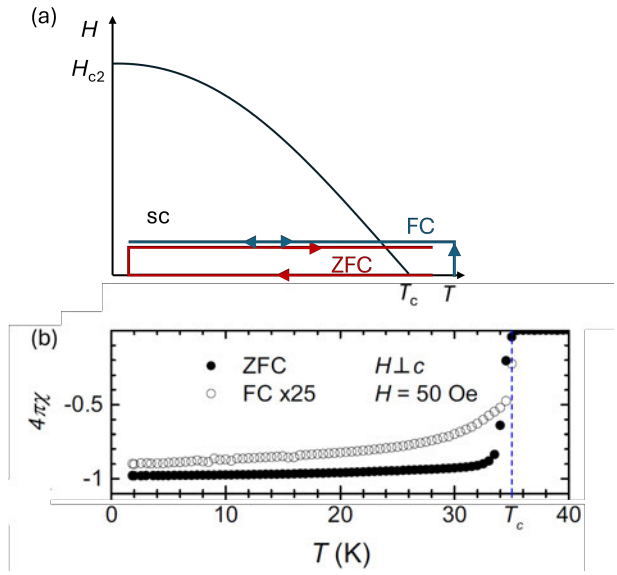

Fig. 10: *(a) Paths in the temperature-field plane that correspond to a field-cooled (FC) and zero-field cooled (ZFC) magnetization measurement for a superconductor. (b) Example of a FC and ZFC measurement. Note that the FC data is multiplied by a factor of 25. (b) Adapted from Ref. [30].*

would show a susceptibility of −1, as the superconducting outer layer already shields the inside. Therefore, the value of the susceptibility in such an experiment is more appropriately called superconducting shielding fraction and should not be called superconducting volume faction (as is often the case). In the end, observation of full magnetic flux expulsion is often intrinsically hampered by vortex pinning, and a well-measured shielding fraction of −1 is an indication for superconductivity, but not a definite proof.

The third important quantity to experimentally prove superconductivity in a material is the heat capacity. It is intrinsically a probe of the sample volume. A heat capacity curve similar to the classic curve derived in BCS theory is a tell-tale sign of a homogeneous superconductor. Two quantities are particularly important: First, the size of the step in heat capacity should be of the order of γT_c (BCS value: $\Delta C_p = 1.43\gamma T_c$, though 'strong-coupling' can increase this value and multi-band superconductivity can decrease it). If the Sommerfeld coefficient γ can be determined, this is an extremely useful sign for true bulk superconductivity. Second, the low-temperature limit of the heat capacity C/T should approach zero, which proves a fully gapped superconducting state. While there are cases when a superconductor intrinsically has a finite C/T in the zero temperature limit, more often this is a sign of sample inhomogeneity. However, a pitfall here is that the electronic heat capacity is added to a phonon background which is often too large to subtract accurately, so that the comparison with the BCS curve is difficult.

Overall, only a combination of different techniques can unambiguously prove superconductivity (zero-resistance, strong diamagnetism and BCS-like heat capacity). Some of these are difficult to implement in specific cases (e.g., under applied pressure) so that this classic trio may not be applied and a clear identification of superconductivity can be hard work, though not impossible.

There are many more 'exotic' order parameters, whose identification needs creative and knowledgeable usage of the wide range of techniques of solid-state physics. To give just one example, 'ferroaxial order' was recently proposed to be identified using specific elastotransport coefficients [36–38]

On concluding this section, I want to mention a famous case where the identification of the order parameter of a phase has eluded the community for almost 40 years and up to date, even though the presence of a phase transition is crystal clear [39]. In URu_2Si_2, a second-order phase transition is clearly observed at $T_{\rm HO} = 17$ K [40]. The heat capacity shows a large step, resistance and magnetization show clear anomalies and phase lines can be clearly followed on applied pressure or magnetic field. However, this phase is shown to neither magnetic order, nor superconductivity (the material becomes superconducting at a much lower temperature) and also not a structural phase transition. Many other order parameters have been proposed but could not be experimentally confirmed [39]. Indeed, it seems that all imaginable techniques of solid-state physics have been thrown at this problem, and the phase still remains unidentified. It is aptly named "hidden order".

4.2 Determination of magnetic and structural order parameters in iron-based superconductors

The family of iron-based superconductors provides interesting examples for the determination of structural and antiferromagnetic order parameters. After the identification of higher-temperature phase transitions in the iron-based superconductors, some signatures of which were noted in the discovery paper in 2008 [10], a concerted effort lead to the determination of the nature of the order parameters. As LaFeAsO was the first material in the family to be studied, here the identification was attempted first and proceeded quickly. Some evidence for a stripe-type antiferromagnetic order was presented only months after the discovery [41]. And slightly later only, neutron diffraction confirmed the stripe-type antiferromagnetic order ("spin density wave") in LaFeAsO [42]. The same work also identified a tetragonal-to-orthorhombic structural transition about 15 K higher than the antiferromagnetic transition. Similarly, diffraction was employed to determine the nature of the ordered phases in $Ba(Fe_{1-x}Co_x)_2As_2$ [43], which turned out to be analogous. Figure 11 presents schematically this stripe-type antiferromagnetic phase and the related tetragonal-to-orthorhombic structural distortion. Yet, the determination of ordered phases proved to be more complex in other iron-based systems.

In FeSe under pressure, two phase transitions (apart from superconductivity) were also identified. The tetragonal-to-orthorhombic structural transition is also present at ambient pressure. The electrical resistance data showed that this transition is suppressed by applied pressure and, eventually, x-ray diffraction could determine the evolution of the structural distortion as a function of temperature and pressure [45, 25]. A second phase transition was shown to emerge under applied pressure. Local magnetic probes such as NMR [46, 47], μSR [22] and time-domain Mössbauer spectroscopy [45] clearly showed that this phase is antiferromagnetic in nature. They also showed indications for stripe-type magnetic order (e.g., [48, 49]). However,

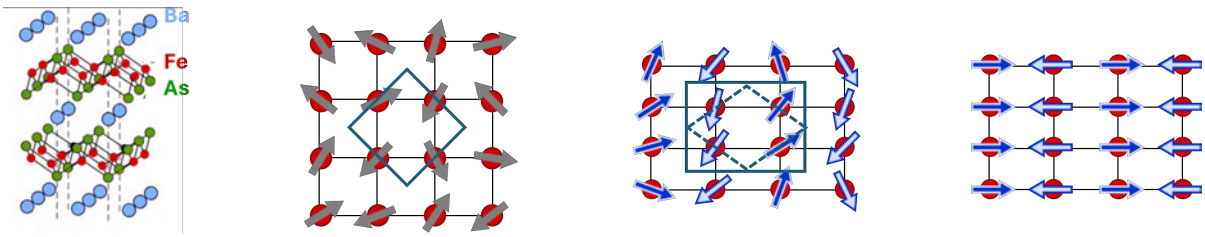

Fig. 11: *Depiction of the characteristic phase transitions in iron-based materials. (a) Sketch of the crystal structure with the Fe atoms indicated in red. (b) View of the Fe plane in the tetragonal paramagnetic state. The unit cell is indicated by the turquoise square, Fe-Fe bonds by black lines. (c) The orthorhombic state with arises from a distortion of the tetragonal unit cell. The "old" unit cell is indicated as the dashed line. The orthorhombic unit cell is twice as large and indicated by the continuous line. (d) Sketch of the stripe-type antiferromagnetic state. Figure adapted from [44].*

unambiguous determination of the magnetic order and its **Q**-vector from a diffraction technique could not be obtained yet. Magnetic neutron diffraction could not resolve the antiferromagnetic phase, most likely due to a combination of small available samples and small ordered moments. FeSe also shows a phase transition to a completely different crystal structure, which is unrelated to electronic correlations but "terminates" the phase diagram [25].
Other interesting magnetic phases were also identified in the iron-based materials. In the determination of all of these phases, theoretical predictions guided the experiments by proposing likely order parameters. Yet, the experiment always has the final say. A small phase pocket of a tetragonal magnetic phase was found in hole-doped iron-based superconductors, such as $Sr_{1-x}K_xFe_2As_2$ [50] (after transport measurements indicated the same feature in pressurized samples [51]). Even though this phase is antiferromagnetically ordered, it turned out to be an example where neutron diffraction alone was not able to uniquely identify the order parameter. In this case, Mössbauer spectroscopy, a local magnetic probe, was the decisive experiment to identify the phase [52]. The new phase corresponds to a superposition of two magnetic order parameters with different **Q**-vectors (see Fig. 12). Neutron diffraction cannot easily differentiate between such a phase and a phase in which the sample splits into different domains, in each of which the order parameter only has a single **Q**-vector.
Finally, we will discuss the identification of another type of magnetic order. It occurs in Co and Ni substituted $CaKFe_4As_4$ [8]. In this material, a phase transition was identified by a subtle kink in resistance at around 50 K. Heat capacity showed a tiny second-order jump. No anomaly in magnetization could be resolved. So, there was clear proof for a well-defined phase transition but the order parameter remained to be identified. Meier et al. [8], used a variety of techniques alongside guidance from theoretical modeling (see Fig. 13).

- Single-crystal x-ray diffraction showed neither the emergence of superstructure peaks (so no doubling, etc., of the unit cell), nor splitting or change in peak profiles which would indicate a distortion of the unit cell. Thus, a structural phase transition was excluded.

- Mössbauer spectroscopy proved the presence of an in-plane hyperfine field at the Fe sites, and indicated that all Fe atoms feel the same value of the hyperfine field.

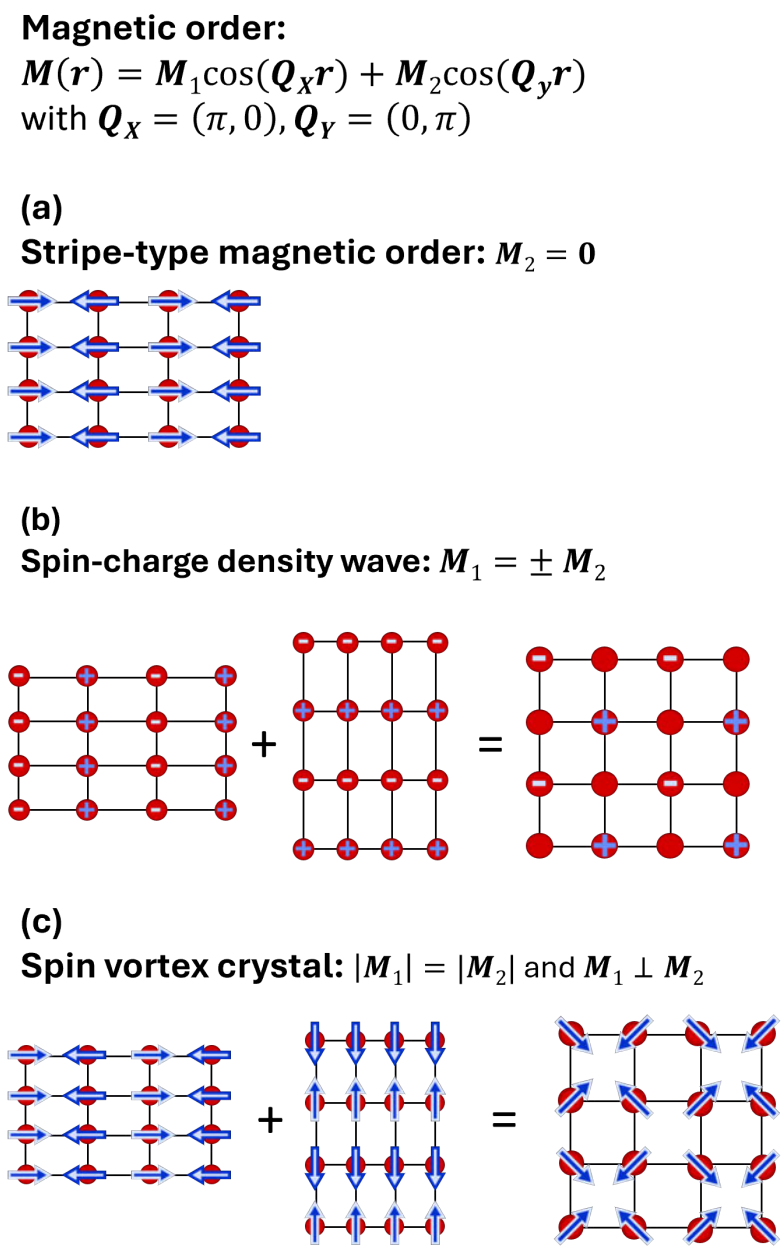

Fig. 12: *Complex magnetic orders realized in iron-based materials, the generally "multi-Q" order parameter is noted. (a) Stripe-type magnetic state with a "single-Q" order parameter. (b) Spin-charge density wave state, which can be seen as a superposition of two stripe-type orders with different Q. (c) Depiction of the so-called spin-vortex crystal state realized in substituted* $CaKFe_4As_4$.

- Nuclear magnetic resonance showed that half of the As nuclei experience no hyperfine field, while the other half experiences a hyperfine field along the c-axis with alternating direction.

From the six likely magnetic orders proposed by theoretical modeling, only one is consistent with these observations. Thus, the so-called spin-vortex crystal magnetic order [see Fig. 12(c)] was determined in Ni-substituted $CaKFe_4As_4$ [8]. Note that an unbiased symmetry analysis is possible based on the fact that the transition is of second-order nature. Therefore, the symmetry

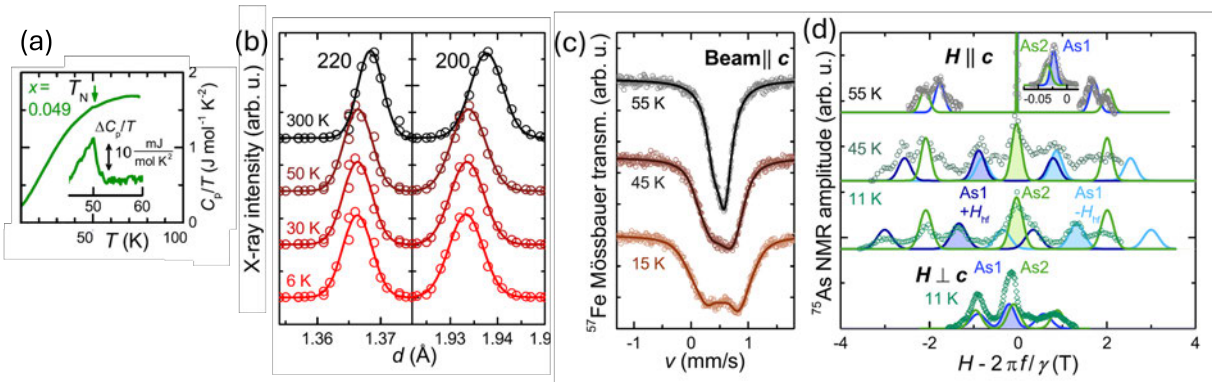

Fig. 13: *Data permitting the identification of the spin-vortex crystal magnetic phase in $Ca(Fe_{0.951}Ni_{0.049})_4As_4$. (a) Heat capacity (b) X-ray diffraction (c) Mössbauer spectroscopy and (d) nuclear magnetic resonance. Figure adapted from Ref. [53].*

group of the low-temperature phase has to differ from the symmetry group of the parent phase by the loss of a single symmetry element. Then, all possible magnetic groups that correspond to the reduction of the parent symmetry group by one element are examined and checked for their consistency with the experimental results [54]. This approach also leads the conclusion of the spin-vortex crystal magnetic phase.

Finally, neutron scattering was performed and confirmed the ordered state to be the hedgehog spin-vortex crystal centered on the As1 atom, with alternate stacking along the c-axis, completely in agreement with the previous conclusions [55].

5 Concluding remarks

The identification of phase transitions and the determination of the corresponding order parameters is a central topic in condensed matter physics. Electronic correlations can lead to structural, magnetic, superconducting, or other "exotic" phase transitions, and a rich phenomenology. There are many experimental and theoretical techniques to experimentally characterize phase transitions and ordered phases, all with their own strengths and pitfalls. In some cases, long-standing and niche techniques may provide a breakthrough while new techniques are continuously being developed and optimized. It is an important skill to find the right technique for the problem at hand, given restrictions, e.g., on available samples and necessary experimental conditions. Such an effort is of high value as the knowledge of its phase diagram is the basis for understanding a correlated-electron material.

References

[1] L.D. Landau and E.M. Lifschitz: *Lehrbuch der Theoretischen Physik V: Statistische Physik* (Akademie Verlag, Berlin, 1975) Chapter VIII

[2] Wikipedia: *Phasendiagramm* Online; accessed 01-July-2026 `https://de.wikipedia.org/wiki/Phasendiagramm`

[3] L.D. Landau and E.M. Lifschitz: *Lehrbuch der Theoretischen Physik V: Statistische Physik* (Akademie Verlag, Berlin, 1975) Chapter XIV

[4] S.K. Yip, T. Li, and P. Kumar, Phys. Rev. B **43** (1991)

[5] V. Taufour, U.S. Kaluarachchi, and V.G. Kogan, Phys. Rev. B **94**, 060410(R) (2016)

[6] K. Semeniuk, D. Hafner, P. Khanenko, T. Lühmann, J. Banda, J.F. Landaeta, C. Geibel, S. Khim, E. Hassinger, and M. Brando, Phys. Rev. B **107**, L220504 (2023)

[7] A.E. Böhmer, F. Hardy, L. Wang, T. Wolf, P. Schweiss, and C. Meingast, Nat. Commun. **6**, 8911 (2015)

[8] W.R. Meier, Q.-P. Ding, A. Kreyssig, S.L. Bud'ko, A. Sapkota, K. Kothapalli, V. Borisov, R. Valentí, C.D. Batista, P.P. Orth, R.M. Fernandes, A.I. Goldman, Y. Furukawa, A.E. Böhmer, and P.C. Canfield, npj Quantum Mater. **3**, 5 (2018)

[9] E. Gati, M. Garst, R.S. Manna, U. Tutsch, B. Wolf, L. Bartosch, H. Schubert, T. Sasaki, J.A. Schlueter, and M. Lang, Sci. Adv. **2**, e1601646 (2016)

[10] Y. Kamihara, T. Watanabe, M. Hirano, and H. Hosono, J. Am. Chem. Soc. **130**, 3296 (2008)

[11] N. Ni, M.E. Tillman, J.-Q. Yan, A. Kracher, S.T. Hannahs, S.L. Bud'ko, and P.C. Canfield, Phys. Rev. B **78**, 214515 (2008)

[12] J.-H. Chu, J.G. Analytis, C. Kucharczyk, and I.R. Fisher, Phys. Rev. B **79**, 014506 (2009)

[13] C. Meingast, F. Hardy, R. Heid, P. Adelmann, A. Böhmer, P. Burger, D. Ernst, R. Fromknecht, P. Schweiss, and T. Wolf, Phys. Rev. Lett. **108**, 177004 (2012)

[14] R.M. Fernandes, D.K. Pratt, W. Tian, J. Zarestky, A. Kreyssig, S. Nandi, M.G. Kim, A. Thaler, N. Ni, P.C. Canfield, R.J. McQueeney, J. Schmalian, and A.I. Goldman, Phys. Rev. B **81**, 140501 (2010)

[15] R.M. Fernandes, A.V. Chubukov, J. Knolle, I. Eremin, and J. Schmalian, Phys. Rev. B **85**, 024534 (2012)

[16] S. Medvedev, T.M. McQueen, I.A. Troyan, T. Palasyuk, M.I. Eremets, R.J. Cava, S. Naghavi, F. Casper, V. Ksenofontov, G. Wortmann, and C. Felser, Nat. Mater. **8**, 630 (2009)

[17] K. Miyoshi, K. Morishita, E. Mutou, M. Kondo, O. Seida, K. Fujiwara, J. Takeuchi, and S. Nishigori, J. Phys. Soc. Jpn. **83**, 013702 (2014)

[18] T. Terashima, N. Kikugawa, S. Kasahara, T. Watashige, T. Shibauchi, Y. Matsuda, T. Wolf, A.E. Böhmer, F. Hardy, C. Meingast, H. v. Löhneysen, and S. Uji, J. Phys. Soc. Jpn. **84**, 063701 (2015)

[19] J.P. Sun, K. Matsuura, G.Z. Ye, Y. Mizukami, M. Shimozawa, K. Matsubayashi, M. Yamashita, T. Watashige, S. Kasahara, Y. Matsuda, J.Q. Yan, B.C. Sales, Y. Uwatoko, J.G. Cheng, and T. Shibauchi, Nat. Commun. **7**, 12146 (2016)

[20] Y. Zheng, Y. Wang, F. Hardy, A.E. Böhmer, T. Wolf, C. Meingast, and R. Lortz, Phys. Rev. B **89**, 054514 (2014)

[21] A.E. Böhmer and A. Kreisel, J. Phys.: Condens. Matter **30**, 023001 (2018)

[22] M. Bendele, A. Amato, K. Conder, M. Elender, H. Keller, H.-H. Klauss, H. Luetkens, E. Pomjakushina, A. Raselli, and R. Khasanov, Phys. Rev. Lett. **104**, 087003 (2010)

[23] K. Cho, M. Kończykowski, S. Teknowijoyo, M.A. Tanatar, J. Guss, P.B. Gartin, J.M. Wilde, A. Kreyssig, R.J. McQueeney, A.I. Goldman, V. Mishra, P.J. Hirschfeld, and R. Prozorov, Nat. Commun. **9**, 2796 (2018)

[24] A. Kogar, A. Zong, P.E. Dolgirev, X. Shen, J. Straquadine, Y.-Q. Bie, X. Wang, T. Rohwer, I.-C. Tung, Y. Yang, R. Li, J. Yang, S. Weathersby, S. Park, M.E. Kozina, E.J. Sie, H. Wen, P. Jarillo-Herrero, I.R. Fisher, X. Wang, and N. Gedik, Nat. Phys. **16**, 159 (2020)

[25] A.E. Böhmer, K. Kothapalli, W.T. Jayasekara, J.M. Wilde, B. Li, A. Sapkota, B.G. Ueland, P. Das, Y. Xiao, W. Bi, J. Zhao, E.E. Alp, S.L. Bud'ko, P.C. Canfield, A.I. Goldman, and A. Kreyssig, Phys. Rev. B **100**, 064515 (2019)

[26] S. Mugiraneza and A.M. Hallas, Commun. Phys. **5**, 95 (2022)

[27] D.C. Johnston, Phys. Rev. B **91**, 064427 (2015)

[28] A. Arrott, Phys. Rev. **108**, 1394 (1957)

[29] G. Drachuck, A.E. Böhmer, S.L. Bud'ko, and P.C. Canfield, J. Magn. Magn. Mater. **417**, 420 (2016)

[30] W.R. Meier, T. Kong, U.S. Kaluarachchi, V. Taufour, N.H. Jo, G. Drachuck, A.E. Böhmer, S.M. Saunders, A. Sapkota, A. Kreyssig, M.A. Tanatar, R. Prozorov, A.I. Goldman, F.F. Balakirev, A. Gurevich, S.L. Bud'ko, and P.C. Canfield, Phys. Rev. B **94**, 064501 (2016)

[31] N.S. Sangeetha, S. Pakhira, Q.-P. Ding, L. Krause, H.-C. Lee, V. Smetana, A.-V. Mudring, B.B. Iversen, Y. Furukawa, and D.C. Johnston, Proc. Natl. Acad. Sci. USA **118**, e2108724118 (2021)

[32] A.E. Böhmer, F. Hardy, F. Eilers, D. Ernst, P. Adelmann, P. Schweiss, T. Wolf, and C. Meingast, Phys. Rev. B **87**, 180505 (2013)

[33] S. Lee, J.-H. Kim, and Y.-W. Kwon: *The First Room-Temperature Ambient-Pressure Superconductor*, arXiv:2307.12008 (2023)

[34] E.A. Yelland, S.M. Hayden, S.J.C. Yates, C. Pfleiderer, M. Uhlarz, R. Vollmer, H. v. Löhneysen, N.R. Bernhoeft, R.P. Smith, S.S. Saxena, and N. Kimura, Phys. Rev. B **72**, 214523 (2005)

[35] A.E. Böhmer, A. Sapkota, A. Kreyssig, S.L. Bud'ko, G. Drachuck, S.M. Saunders, A.I. Goldman, and P.C. Canfield, Phys. Rev. Lett. **118**, 107002 (2017)

[36] E. Day-Roberts, R.M. Fernandes, and T. Birol, Phys. Rev. Lett. **134**, 016401 (2025)

[37] Q. Jiang, E. Day-Roberts, B. Gonzalez, A. Das, D.H. Torchinsky, T. Birol, R.M. Fernandes, and I.R. Fisher: *Evidence for ferroaxial order in 1T-$TiSe_2$ via elastoresistivity measurements* arXiv:2603.14613 (2026)

[38] S. Edwards, E. Rosenberg, I. Maccari, J. Wen, C. Hu, X. Xu, J.-W. Kim, P.J. Ryan, R.M. Fernandes, F. de Juan, M.N. Gastiasoro, and J.-H. Chu: *Ferroaxial and nematic transitions in the charge density wave phase of 1T-$TiSe_2$*, arXiv:2603.14614 (2026)

[39] J. Mydosh and P. Oppeneer, Phil. Mag. **94**, 3642 (2014)

[40] T.T.M. Palstra, A.A. Menovsky, J. v. d. Berg, A.J. Dirkmaat, P.H. Kes, G.J. Nieuwenhuys, and J.A. Mydosh, Phys. Rev. Lett. **55**, 2727 (1985)

[41] J. Dong, H.J. Zhang, G. Xu, Z. Li, G. Li, W.Z. Hu, D. Wu, G.F. Chen, X. Dai, J.L. Luo, Z. Fang, and N.L. Wang, Europhys. Lett. **83**, 27006 (2008)

[42] C. de la Cruz, Q. Huang, J.W. Lynn, J. Li, W.R. II, J.L. Zarestky, H.A. Mook, G.F. Chen, J.L. Luo, N.L. Wang, and P. Dai, Nature **453**, 899 (2008)

[43] D.K. Pratt, W. Tian, A. Kreyssig, J.L. Zarestky, S. Nandi, N. Ni, S.L. Bud'ko, P.C. Canfield, A.I. Goldman, and R.J. McQueeney, Phys. Rev. Lett. **103**, 087001 (2009)

[44] A. Böhmer and A. Kreyssig, Physik in unserer Zeit **48**, 70 (2017)

[45] K. Kothapalli, A.E. Böhmer, W.T. Jayasekara, B.G. Ueland, P. Das, A. Sapkota, V. Taufour, Y. Xiao, E.E. Alp, S.L. Bud'ko, P.C. Canfield, A. Kreyssig, and A.I. Goldman, Nat. Commun. **7**, 12728 (2016)

[46] T. Imai, K. Ahilan, F.L. Ning, T.M. McQueen, and R.J. Cava,
Phys. Rev. Lett. **102**, 177005 (2009)

[47] K. Rana and Y. Furukawa, Front. Phys. **10**, 849284 (2022)

[48] P. Wiecki, M. Nandi, A.E. Böhmer, S.L. Bud'ko, P.C. Canfield, and Y. Furukawa,
Phys. Rev. B **96**, 180502 (2017)

[49] R. Khasanov, Z. Guguchia, A. Amato, E. Morenzoni, X. Dong, F. Zhou, and Z. Zhao,
Phys. Rev. B **95**, 180504(R) (2017)

[50] S. Avci, O. Chmaissem, J. Allred, S. Rosenkranz, I. Eremin, A. Chubukov, D. Bugaris, D. Chung, M. Kanatzidis, J.-P. Castellan, J. Schlueter, H. Claus, D. Khalyavin, P. Manuel, A. Daoud-Aladine, and R. Osborn, Nat. Commun. **5**, 3845 (2014)

[51] E. Hassinger, G. Gredat, F. Valade, S.R. de Cotret, A. Juneau-Fecteau, J.-P. Reid, H. Kim, M.A. Tanatar, R. Prozorov, B. Shen, H.-H. Wen, N. Doiron-Leyraud, and L. Taillefer, Phys. Rev. B **86**, 140502 (2012)

[52] J.M. Allred, K.M. Taddei, D.E. Bugaris, M.J. Krogstad, S.H. Lapidus, D.Y. Chung, H. Claus, M. Kanatzidis, D.E. Brown, J. Kang, R.M. Fernandes, I. Eremin, S. Rosenkranz, O. Chmaissem, and R. Osborn, Nat. Phys. **12** (2016)

[53] W.R. Meier, T. Kong, S.L. Bud'ko, and P.C. Canfield, Phys. Rev. Mater. **1**, 013401 (2017)

[54] W.R. Meier: *Growth, properties and magnetism of* $CaKFe_4As_4$
(PhD thesis, Iowa State University, 2018)

[55] A. Kreyssig, J.M. Wilde, A.E. Böhmer, W. Tian, W.R. Meier, B. Li, B.G. Ueland, M. Xu, S.L. Bud'ko, P.C. Canfield, R.J. McQueeney, and A.I. Goldman,
Phys. Rev. B **97**, 224521 (2018)